

Characterization of a fibre optic swept laser source at 1 μm for optical coherence tomography imaging systems

Irina Trifanov^a, Liviu Neagu^b, Adrian Bradu^b, Antonio Lobo Ribeiro^c, Adrian Gh. Podoleanu^b

^aMultiwave Photonics S.A., R. Eng. Frederico Ulrich 2650,
4470-605 Moreira da Maia, Portugal

^bApplied Optics Group, School of Physical Sciences, University of Kent,
CT2 7NH Canterbury, United Kingdom

^cFaculty of Health Sciences, University Fernando Pessoa,
R. Carlos da Maia 296, 4200-150 Porto, Portugal

ABSTRACT

We report the development of a swept wavelength laser at 1 micron based on a linear cavity fibre configuration with an intra-cavity half symmetrical confocal Fabry-Perot tunable filter and a semiconductor optical amplifier as a gain medium. The performances of the source in terms of parameters like: sweep repetition rate (1-20 kHz), center wavelength (1065 nm), wavelength scanning range (max. 50nm), instantaneous line-width (<0.1nm) and a boosted output power of around 40 mW are demonstrated. The new source tested on an OCT system is exhibiting sufficient linearity in wave-number (k-space) at 1 kHz repetition rate; therefore no k-trigger, or wavelength rescaling process was needed.

Keywords: optical coherence tomography, swept source, SOA, Fabry-Perot filter

1. INTRODUCTION

Most wavelength swept laser sources that use a scanning Fabry-Perot filter or a diffraction grating with a resonant mirror have a nonlinear, sinusoidal temporal change of frequency due to the typically sinusoidal excitation of the piezo controller in the laser cavity. A proper depth profile can be obtained only by re-sampling or recalibrating the detected OCT interference-fringe signals prior to Fast Fourier transformation (FFT), in order to provide data evenly sampled in optical frequency. Incorrect wavelength mapping generates a depth dependent broadening of the PSF similar to dispersion in OCT images. Moreover, a highly nonlinear tuning curve is undesirable as it complicates the linearization process and requires higher computation times.

For a linear optical frequency tuning of a swept source illuminating an interferometer, the interferogram produced by the interferometer should be perfectly periodic, with the beating frequency proportional to the optical path difference (OPD). For a sinusoidal oscillation, the phase, or the argument of the sinusoidal oscillation, is linearly related to the wavenumber k .

Any nonlinearity in the sweep of the optical frequency reflects in a nonlinear dependence of the phase on the wavenumber. Consequently, by using a processing algorithm to retrieve the optical phase can allow a proper evaluation of the linearity of a swept source.

Our observation was that for a linear excitation of the filter in the form of a ramp or saw tooth waveform at a slow frequency sweep (around 1 kHz), the instantaneous frequency generated varied linearly in time. We termed such response as sufficiently linear. The source has been integrated into an OCT imaging system and characterized in terms of: sensitivity, axial resolution and ranging depth.

2. MATERIALS AND METHODS

Figure 1 depicts a schematic of the fibre wavelength swept laser source. A linear-cavity configuration was chosen. It consists of a fibre coupled semiconductor amplifier (SOA from Superlum) as a gain medium, a piezoelectric fibre coupled Fabry-Perot tunable filter (FFP-TF from LambdaQuest), a polarisation maintaining (PM) fibre mirror as a back reflector, a PM circulator and a PM fibre output coupler. Linear cavity has the advantage that the gain medium amplifies the laser light twice per circulation, making it easy to reach deep saturation, whereas its disadvantage resides in less stable laser oscillations due to the backward reflected light from intra-cavity components. As shown in Fig. 1, the radiation propagates twice through the gain medium and only once through the loop, therefore reducing the insertion losses introduced by these components by two fold. The SOA has a -3 dB optical gain bandwidth, a small signal gain of 25 dB and a saturation output power of 12 dBm. The tunable filter consists of two highly reflective surfaces where one is designed as a concave surface fabricated on the end of a fiber. The concave mirror aligned to the fiber core has its curvature matched to that of the incoming waveform. This confocal design simplifies angular alignment and reduces vibration sensitivity [1]. The filter exhibits a free spectral range of 75 nm, a line-width of ~12 nm and an insertion loss of ~2.5 dB.

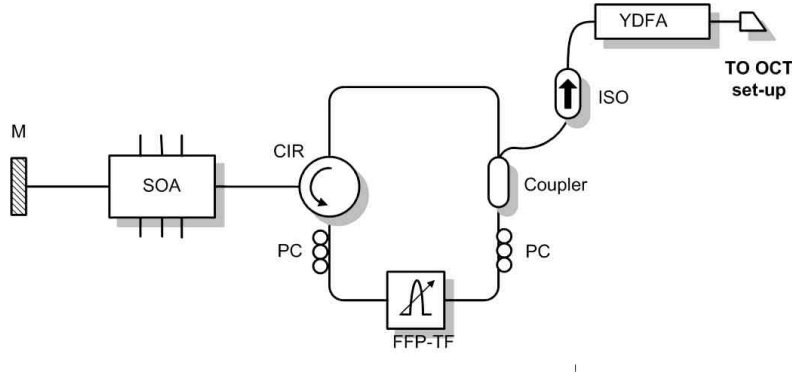


Figure 1. Schematic of the amplified frequency swept laser source.

The laser output is coupled out via a 50/50 coupler. After isolation, the output is amplified using a PM Ytterbium doped fiber amplifier (YDFA, from Multiwave Photonics) operating in the 1030 - 1080 nm wavelength band with a 17 dB small signal gain and a saturated output power of 50 mW. The optical amplifier includes input and output isolators, as well as high quality linear polarizers that block the power in the fast axis, ensuring a polarization extinction ratio over 25 dB at the output.

Figure 1a shows the peak hold mode spectrum of the amplified wavelength swept laser with a full width maximum range of ~ 50 nm and 49 mW output power, limited by the SOA gain properties. The time domain output trace is shown in Figure 1b. The ramp applied to the tunable filter is chosen to have positive saw-tooth scanning from short wavelength to long wavelength, since the reverse-sweep induces nonlinear effects in the SOA, lowering laser output power [2].

We have theoretically estimated the maximum frequency sweep in the saturation regime, that is set by the effective number of roundtrips required for the gain medium to reach saturation before the filter has changed position as expressed in eq. (1) from reference [3].

$$f_{sweep}^{\max} = \frac{\delta\lambda \cdot \log(G \cdot \rho) \cdot c}{\Delta\lambda \cdot \log\left(\frac{P_{sat} \cdot \Delta\lambda}{P_{Asat} \cdot \delta\lambda}\right) \cdot n \cdot L} \quad (1)$$

The length of the cavity $L = 9$ m and $T_{roundtrip} = 43.5$ ns were indirectly calculated from the longitudinal mode spacing. Assuming a 30 dB gain ($G = 1000$) of the SOA, $\rho = 0.1$, $P_{sat} = 15.7$ mW, $P_{ASEtotal} = 5$ mW will give a saturation build up limit for a ramp waveform of $f_{sweep} = 27.47$ kHz. Shorter cavity length is desired to facilitate rapid scanning, i.e. a reduction of the cavity length by two-fold will improve the sweeping frequency by a factor of 2.

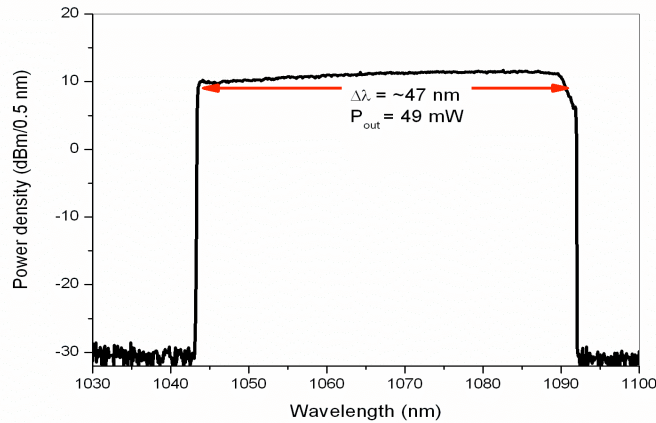


Fig. 2: Peak hold mode spectrum of the amplified swept laser source.

The OCT system, shown in Figure 3, uses a dual balance detection scheme for recording the interferogram from the interferometer on a high speed analog-to-digital converter (A/D) operating at 200 MSamples/s with 12-bit resolution (National Instruments, model NI 5124). The high sampling rate of the digitizer ensures very high acquisition rates of the B-scan images. Thus, if 4000 points are used to digitize each sweep, we have the potential to produce 50,000 sweeps per second. Hence, for a B-scan image made of 500 consecutive A-scans, frame rates up to 100 Hz could in principle be achieved, if the swept source is fast enough. In our particular case, at 1 kHz sweeping speed, the maximum achievable frame rate when 500 A-scans are used to build each B-scan would be 0.5 Hz.

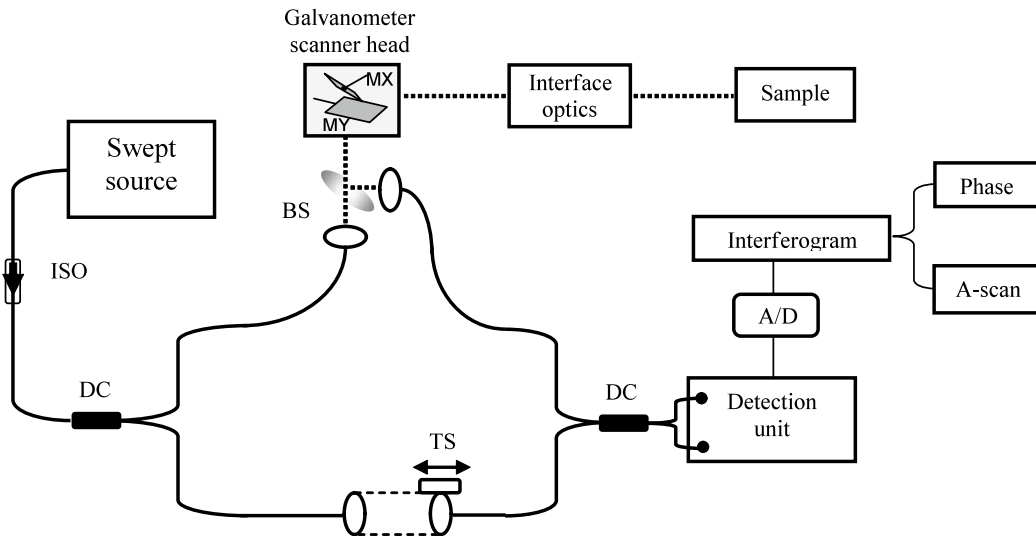


Figure 3. Schematic of the interferometric OCT set-up configured as a Mach-Zehnder interferometer using directional fibre couplers (DC). Part of the radiation from the source is sent, via a bulk beam-splitter (BS), to the interferometer sample-arm, comprising of a pair of orthogonal galvo-scanners and interface optics for imaging. The backscattered signal from the sample is coherently recombined with the interferometer reference-arm at the detector. The optical path difference (OPD) is adjusted using a translation stage (TS).

3. RESULTS

A typical interferogram is shown in Figure 4, amplitude (a) and phase (b), obtained for a 1 kHz frequency sweep, where a number of 1600 sampling points per sweep have been used. As the ramp wave-form applied to the filter was 90%, we ended up with approximately 1400 sampling points per sweep. After digitization, the phase of the acquired signal is calculated and a FFT provided the A-scan (reflectivity profile in depth).

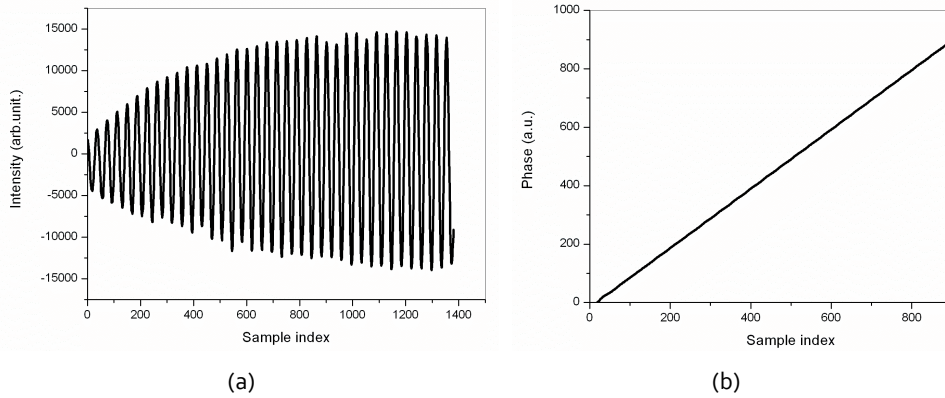


Fig. 4. (a) Spectral interferogram and (b) retrieved spectral phase of the OCT signal for a single amplified laser sweep at 1 kHz.

The *roll-off performance* determines a decrease in the OCT signal strength with ranging depth, caused by the limited instantaneous coherence length of the applied swept light source. This exponential fall-off with depth is quantified conventionally by defining the one side-depth at which the sensitivity falls off by a factor of $\frac{1}{2}$ or 6 dB in amplitude. To characterize the system sensitivity as a function of ranging depth, 1000 A-lines were acquired for 12 different positions of a calibrated reflector placed in the sample arm. The FFT was performed over forward sweeps (0.5 ms) without any numerical re-sampling and apodization. The point spread functions (PSF) obtained are shown in Figure 5 against the OCT ranging depth (i.e. 0.5x arm length mismatch of the Mach-Zehnder interferometer). A 6 dB decrease in signal intensity corresponds to a depth of ~ 3 mm, which represents one half of the coherence length or ~ 0.08 nm laser linewidth.

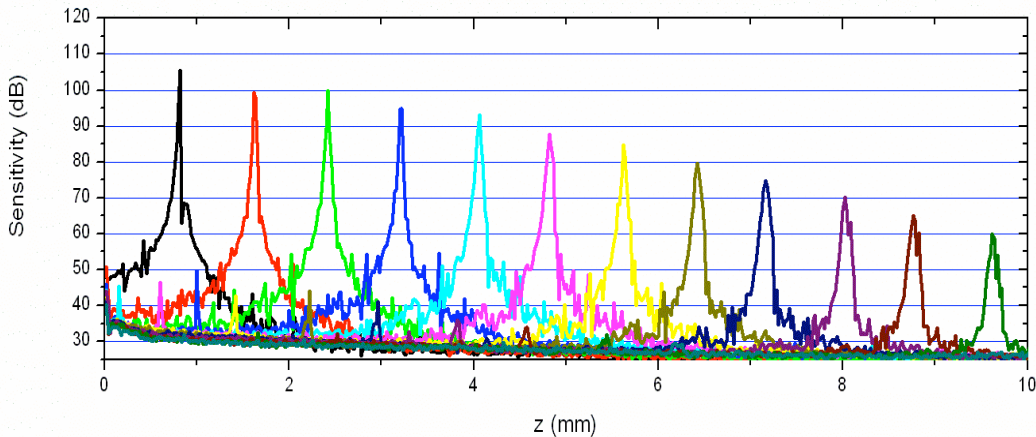


Fig. 5. Measured point spread function (PSF) for different delays (averaging 1000 A-scan per PSF).

Sensitivity: The maximum sensitivity measured was -105.5 dB at 0.8 mm with an average power on the sample of 2.8 mW. This value was obtained by using a calibrated reflector placed in the sample arm (an optical density filter with 12.7 dB attenuation placed in front of a mirror) and observing the resulting SNR of the OCT signal (i.e. peak height to root-mean-squared (RMS) noise). A significant attenuation of the reference power was performed by limiting the aperture of a pinhole placed in the reference beam free path. This suggests that the source exhibits significant relative intensity noise (RIN), which will also limit the detection sensitivity especially for higher imaging speeds.

Axial resolution: A representative of the PSF measured at about 0.9 mm in depth from zero delay point is shown in Figure 6 with a mirror as an object (linear and logarithmic scale, respectively). No linearization procedure was applied. Theoretically, a tuning range of 50 nm (at FWHM) would give about $\sim 10 \mu\text{m}$ resolution in air. The measured value was $\sim 29.0 \mu\text{m}$ in air, close to 0.9 mm delay point. The difference may be due to uncompensated dispersion left in the system as well as small non-linearities in the optical frequency sweep. The measured value was $\sim 20.0 \mu\text{m}$ in air, close to 0.1 mm delay point. The difference accounts for some uncompensated dispersion left in the system as well as non-linearities in the optical frequency sweep.

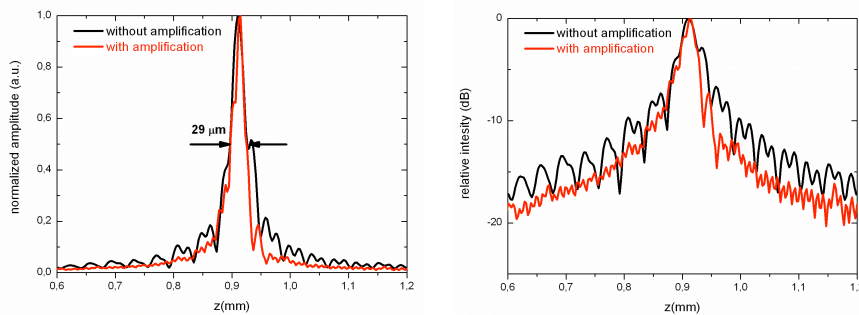


Fig. 6. Measured point spread functions of the OCT system on a linear scale left and on a logarithmic scale (right) with and without laser source amplification.

OCT ranging depth: Figure 7 illustrates a set of B-scan images from a human tooth with lead taken at different depths. Images from more than 5-6 mm depth could be visualized, which corresponds to a sensitivity roll-off point of -20 dB. The OCT ranging depth is much larger than the confocal depth of field of about (2 mm) of the 36 mm objective used, therefore attenuation of signal from depths outside the confocal gate is expected. To compensate for the decay of amplitude signal with depth, electronic gain on the images was applied from one image to the next. In this way, backscattering from locations deeper than 10 mm (measured in air) becomes visible.

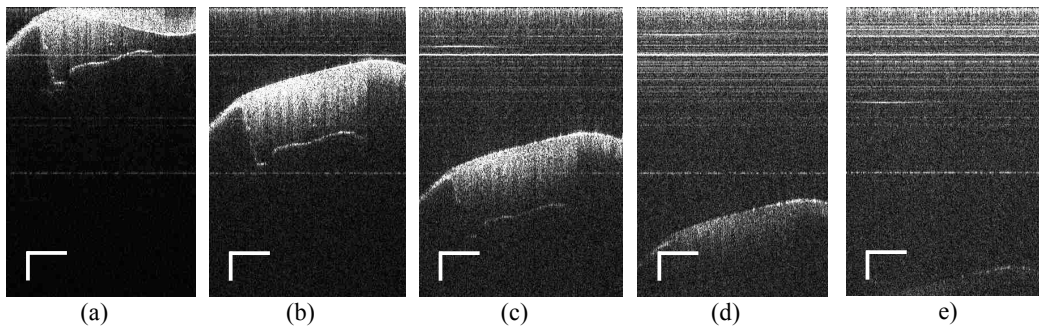


Fig. 7. B-scan OCT images of a human tooth at 5 different depth positions and increased electronic gain. (a): 0 mm, (Gain 0.3); (b) 2.5 mm, (Gain 0.6); (c): 5mm, (Gain 0.9); (d): 7.5mm, (Gain 1.2); (e):10 mm, (Gain 1.5).

Saturation of photo-detectors due to variation of power within the sweeping may determine lines across the image [4]. Most likely, such lines are due to imperfections in the balance detection unit, where the balancing varies with the swept wavelength. A possible solution to eliminate or reduce the intensity of such lines consists in background subtraction (operational as long as no saturation takes place). Unfortunately, such subtraction needed to be performed more than once due to power drifts in the laser.

In the images shown in Figure 8 background subtraction was performed. The images display (a) the same tooth as in Figure 7 and (b) a human finger at the junction between nail and skin.

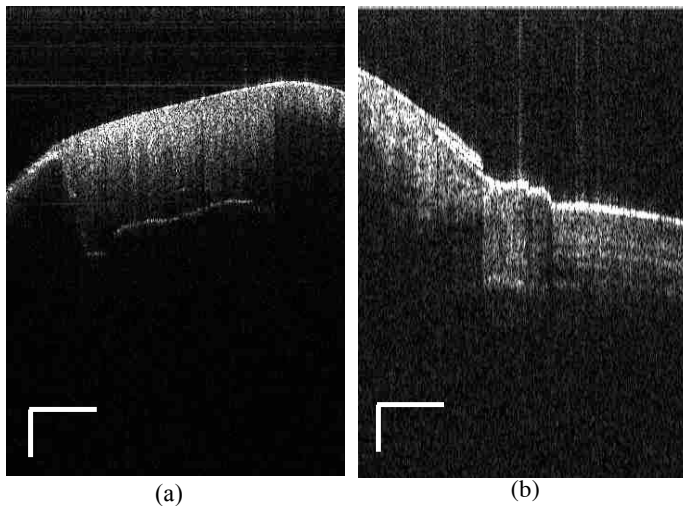


Figure 8. (a) Human tooth with lead. (b) Human finger at the junction between nail and skin. Scale bars represent 1 mm.

4. CONCLUSION

In conclusion, applying a ramp, instead of a sinusoidal waveform signal to the filter at moderate frequency speeds could represent an easy solution for overcoming the nonlinearity for this type of lasers. This is especially suitable as for wavelength swept laser sources the time-constant to build up lasing from ASE background limits the maximum frequency sweep to about ~ 50 kHz). One major issue in applying non-sinusoidal drive waveforms at high frequencies (several 10 kHz) to the FFP-TF is the non-flat phase and amplitude response of the filter and the electronic drive circuitry. Recently, a high linearity in k-space was obtained for a FDML swept source by applying an optimized drive form to account for the filter response function [5]. The same hardware technique could be applied here to enable high linearity that may allow achieving sweep frequencies of around 20-30 kHz.

ACKNOWLEDGEMENTS

Irina Trifanov acknowledges the Marie Curie training site (MEST-CT-2005-02035).

Adrian Bradu and Adrian Podoleanu acknowledge the Engineering and Physical Sciences Research Council (EPSRC) grant EP/H004963/1 and the support of the European Research Council (<http://erc.europa.eu/>) grant 249889.

REFERENCES

1. Y. Yeh, Y. Choi and H. F. Taylor, "A High-Speed Tunable Filter Using a Concave Fiber Mirror," in *Optical Fiber Communication Conference and Exposition and The National Fiber Optic Engineers Conference*, Technical Digest, OSA, paper JWA23, 2005.
2. A. Bilenca, S. H. Yun, G. J. Tearney, and B. E. Bouma, "Numerical study of wavelength-swept semiconductor ring lasers: The role of refractive index nonlinearities in semiconductor optical amplifiers and implications for biomedical imaging applications," *Opt. Lett.*, vol. 31(6), 760–762, 2006.

3. R. Huber, M. Wojtkowski, K. Taira, J. G. Fujimoto, and K. Hsu, "Amplified, frequency swept lasers for frequency domain reflectometry and OCT imaging: design and scaling principles," *Opt. Express* **13**, 3513- 3528, 2005.
4. Kathy Zheng, Bin Liu, Chuanyong Huang, and Mark E. Brezinski, "Experimental confirmation of potential swept source optical coherence tomography performance limitations," *Appl. Opt.* **47**, 6151-6158, 2008.
5. C.M. Eigenwillig, B.R. Biedermann, G.Palte, and R.Huber, "K-space linear Fourier domain mode locked laser and applications for optical coherence tomography," *Opt. Express* **16**, 8916-8937, 2008.